The state filling effect in p-doped InGaAs/GaAs quantum dots

2007 J. Phys.: Condens. Matter 19 386213

(http://iopscience.iop.org/0953-8984/19/38/386213)

IOP PUBLISHING JOURNAL OF PHYSICS: CONDENSED MATTER

J. Phys.: Condens. Matter **19** (2007) 386213 (10pp) doi:10.1088/0953-8984/19/38/386213

The state filling effect in p-doped InGaAs/GaAs quantum dots

X M Wen[1,2], L V Dao[2], P Hannaford[2], S Mokkapati[3], H H Tan[3] and C Jagadish[3]

[1] Department of Physics, Yunnan University, Kunming, Yunnan 650091, People's Republic of China
[2] Centre for Atom Optics and Ultrafast Spectroscopy, Swinburne University of Technology, Melbourne 3122, Australia
[3] Department of Electronic Materials and Engineering, Research School of Physical Sciences and Engineering, The Australian National University, Canberra 0200, Australia

E-mail: xwen@swin.edu.au

Received 11 April 2007, in final form 24 July 2007
Published 31 August 2007
Online at stacks.iop.org/JPhysCM/19/386213

Abstract

The electron dynamics in modulation p-doped InGaAs/GaAs self-assembled quantum dots have been studied by time-integrated and time-resolved up-conversion photoluminescence. A significant state filling effect is observed with exclusion of the phonon bottleneck effect. The rise time and decay time are found to vary with the excitation intensity for the ground state and excited states of the quantum dots. In the low intensity regime the rise time decreases with increasing excitation intensity because of the increased scattering between the photoexcited electrons and excess holes. By contrast, in the high excitation regime the rise time exhibits a slight decrease due to the state filling effect. A simplified rate equation model indicates that the modulation p-doped quantum dots exhibit an increasing saturation factor with increasing detection photon energy based on the theory of parabolic confinement of the quantum dots, which is consistent with the observed excitation dependence.

(Some figures in this article are in colour only in the electronic version)

1. Introduction

Semiconductor quantum dots (QDs) have attracted much attention in condensed matter physics in recent years because they are key materials for the next generation of electronic and optoelectronic devices. In particular, p-doped QDs can greatly improve the electrical and optical properties due to their excess built-in holes [1–3]. Non-equilibrium carrier dynamics play an important role in determining the performance limitations of QD lasers and therefore have been the subject of considerable research in recent years [4]. The atomic-like discrete

energy states of QDs are expected to lead to a state filling effect due to the Pauli exclusion principle taking effect when only a few carriers populate the lower states. This will also lead to hindered intersubband relaxation and to the observation of excited-state interband transitions as the excitation intensity is increased. The state filling effect is an interesting phenomenon that has been extensively investigated in various quantum structures using a variety of techniques, and it provides detailed information on the optical and dynamical properties [5, 6].

The state filling effect, phonon bottleneck and segregated inhomogeneous broadening can give rise to higher energy emission peaks, but they possess distinctive characteristic features. The state filling effect is the only one which will show clear saturation effects. In general, the intersubband relaxation is significantly more efficient than the interband recombination of the corresponding excited state if there is no significant phonon bottleneck effect. Thus only the transition from the ground state is observed at low excitation intensity. With increasing excitation intensity, a progressive saturation of the lower energy transitions is combined with the emergence of emission peaks originating from the excited-state interband radiative transitions. The intersubband carrier relaxation toward the lower levels is slowed down due to the reduced number of available final states. By contrast, the phonon bottleneck effect will permit excited-state interband transitions even under low excitation conditions because the intersubband and interband relaxation dynamics are comparable. On the other hand, in the case of segregated inhomogeneous broadening, multiple peaks with the same relative amplitude are usually observed over a broad range of excitation intensity, since they reflect the relative abundance of a given ground-state energy relative to the other available ground-state energies in the probed area. Consequently, in the case of segregated inhomogeneous broadening in quantum wells, the energy position of the peaks can be observed following the energy predicted for a quantum well with a fluctuation of a few monolayers from its mean deposited thickness. By contrast, in self-assembled QDs the energy spectra of the excited states are typically quite different from the monolayer fluctuation energies due to lateral confinement [6].

The observed photoluminescence (PL) peak separation between the radiative recombination of adjacent excited states in self-assembled QDs is typically about 50–80 meV [7, 8]. This allows excited-state transitions to be resolved in the presence of inhomogeneous broadening which for self-assembled QDs typically has a full width at half maximum (FWHM) of similar size. This broadening arises from small fluctuations in the QD size, alloy composition variations, and shifts due to strain-field effects. The major contribution to the inhomogeneous broadening comes from the variation of dot size due to the large confining potentials and the small volumes. However, due to self-organizing processes, segregated inhomogeneous size broadening is not normally observed in InGaAs/GaAs self-assembled QDs. Under favourable growth conditions, alloy fluctuations can be minimized, and would certainly never lead to segregated inhomogeneous alloy broadening under normal conditions [6].

In addition, many-body phenomena such as biexcitons, charge excitons, exciton complexes, and band-gap renormalization can also contribute to the broadening at higher excitation intensities. However, for a large ensemble of QDs they will be difficult to resolve in the presence of the above inhomogeneous broadening mechanisms, as they can only shift the emission energy by a few millielectron volts [9, 10].

The carrier relaxation and capture into quantum dots play a central role in determining the performance of QD lasers; they have been extensively studied in recent years and various relaxation mechanisms have been proposed, such as Auger processes [11], electron–hole interactions [2] and multi-phonon processes [12]. The p-type doping of quantum dots can greatly improve the performance of QD lasers because of effective compensation of the closely spaced hole states [1]. Gündoğdu *et al* [2] found an extremely fast carrier relaxation from the barrier to the ground state in doped InAs QDs, especially in a p-doped sample, which was

attributed to efficient electron–hole scattering. Siegert *et al* [13] studied the carrier dynamics of modulation doped InAs QDs with different excitation conditions to classify the contribution of different mechanisms of carrier relaxation. However, the detail of the relaxation mechanism depends sensitively on the features of the QDs, such as the composition, dot size, doping density, temperature, excitation density and wavelengths, and it is difficult to identify the particular relaxation mechanisms from experiments [14–16].

In this paper, we present investigations of the state filling effect and electron dynamics of p-doped InGaAs/GaAs self-assembled QDs using time-integrated and time-resolved up-conversion photoluminescence techniques at various excitation conditions. In the low and high excitation regimes the different variations of the rise times suggest that different effects, electron–hole scattering and the state filling effect, are the dominant mechanisms. A simplified rate equation model is presented to understand quantitatively the main microscopic processes involved in the observed PL transitions in modulation p-doped QDs based on the theory of parabolic confinement of the QD ensemble.

2. Experimental details

The InGaAs QD sample used in this work was grown on semi-insulating (100) GaAs substrates by low-pressure metalorganic chemical vapour deposition (MOCVD). First, 200 nm of GaAs buffer layer was grown at 650 °C on a semi-isolated GaAs substrate, followed by $In_{0.5}Ga_{0.5}As$ dots grown and capped with 11 nm GaAs at 550 °C. After a 1 min interruption, a 10 nm thick GaAs layer was grown as the temperature was ramped to 650 °C. The quantum dots have base diameters of 20–30 nm and 4–5 nm height, with density of 3×10^{10} cm^{-2}. A 20 nm thick doped GaAs (III/V ratio of 100:40) layer was grown at 650 °C with a CCl_4 flow of 5×10^{-7} Torr; the corresponding doping density is about 5×10^{15} cm^{-3}. Finally, 170 nm undoped GaAs was capped at 650 °C.

The time-resolved PL (TRPL) experiment was performed using the up-conversion technique, similar to that used previously [17]. The QD sample was excited by 800 nm ultrashort pulses with duration 80 fs and repetition rate 1 kHz from a regenerative amplifier. The photoluminescence from the sample was collected in a back-scattering geometry and mixed in a nonlinear β-barium borate (BBO) crystal with a variable delay gating pulse (800 nm, 80 fs, 20 μJ) to generate a sum-frequency mixing signal. The sum-frequency signal was dispersed in a monochromator and detected with a photomultiplier coupled to a lock-in amplifier system. The up-conversion system has a time resolution of 150 fs and a spectral resolution of 2 nm. The time-integrated PL (CWPL) experiment was performed with two kinds of laser excitation. One was a 532 nm laser, which allows continuum excitation with relatively low power. The other was 800 nm ultrashort pulses from a regenerative amplifier that can achieve much higher temporary peak intensity due to the much shorter duration. The PL was measured using a conventional spectrometer and photomultiplier.

3. Results and discussion

The CWPL spectra excited by the 532 nm laser were measured at 77 and 293 K. At 77 K with 2 mW excitation, the CWPL spectrum exhibits a single Gaussian distribution, which can be attributed to the ground-state transition. No evidence of a phonon bottleneck is observed because there is no excited-state component at low excitation. On increasing the excitation to 52 mW, the CWPL spectrum reveals an evident asymmetry on the high-energy side, as shown in the inset of figure 1. The spectrum is fitted well with a two-Gaussian function, and the locations of the ground state and the excited state with an energy separation of 76 meV are

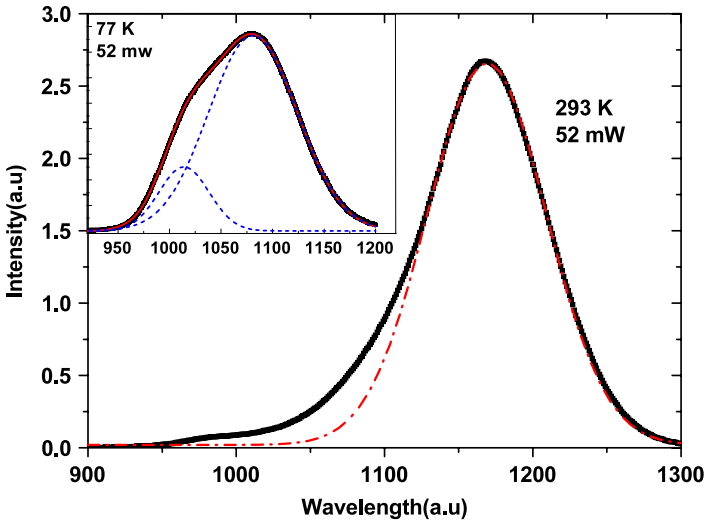

Figure 1. Time-integrated PL spectrum of modulation p-doped InGaAs/GaAs QDs for a 532 nm laser excitation of intensity 52 mW at 293 K. The dotted line indicates a single Gaussian component. The inset shows the PL spectrum with the same excitation at 77 K and a two-Gaussian fit; the dotted lines are the corresponding Gaussian components.

deduced; the corresponding Gaussian components are also shown in the inset (dotted line). These results suggest that saturation takes place in the ground-state transition and there is a comparable contribution from excited-state transitions.

At 293 K with 52 mW excitation, the PL spectrum also shows an asymmetry on the high-energy side, as shown in figure 1. The amplitude of the excited states is much smaller than that of the ground state. Thus the state filling effect is difficult to identify under these excitation conditions because the contribution of the excited states is markedly smaller than that of the ground state, and inhomogeneous broadening is large. The PL component from the second excited state does not appear at low temperature but appears at room temperature, which probably results from the thermal activation at room temperature [13].

Figure 2 shows the PL spectra at various excitation intensities of ultrashort pulses at 293 K. At low excitation intensity, the PL from the ground state is evidently observed, but that from the excited states is hard to distinguish due to extremely weak PL signal and noise from the laser fluctuation. With increasing excitation intensity, in addition to the transitions from the ground state, transitions from the excited states and the wetting layer (WL) are clearly identified, which suggests that the high-energy peaks originate from a state filling effect rather than the phonon bottleneck. In this situation, the intersubband relaxation times of the QDs should be significantly shorter than the lifetime of the excited states, otherwise the excited-state luminescence would be observed even at low excitation intensity (phonon bottleneck effect). With further increasing excitation intensity, the strong state filling effect leads to intense PL from the wetting layer.

Figure 3 shows the evolution of the photoluminescence detected from the ground state (a), the first excited state (b) and the second excited state (c), for an excitation intensity of about 100 μJ cm^{-2}. Each curve is well fitted by the exponential rise and decay function $A[\exp(-t/\tau_{\mathrm{D}}) - \exp(-t/\tau_{\mathrm{R}})]$, where τ_{D} and τ_{R} are the decay time and rise time, respectively. The squares correspond to the experimental data and the solid line represents the fitted curve. We deduce rise times for the ground state of 30 ps and for the excited states of

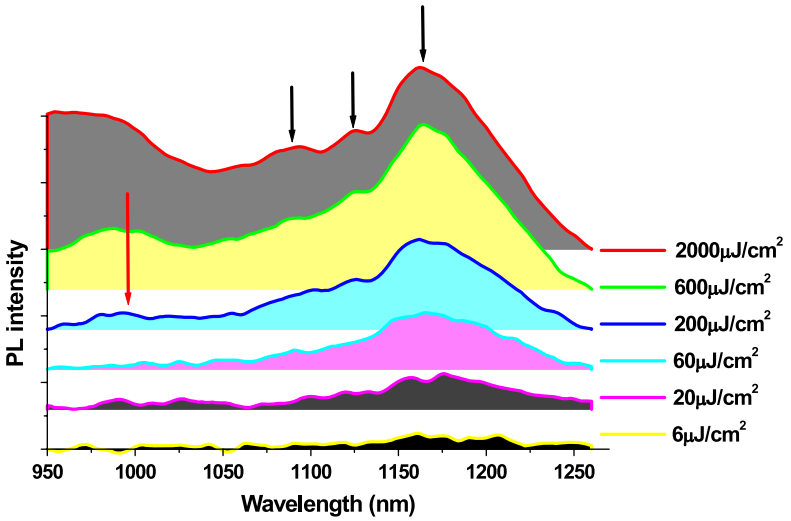

Figure 2. Time-integrated PL spectrum of modulation p-doped InGaAs/GaAs QDs excited at various excitation intensity of an ultrashort pulse at room temperature. The arrows indicate the transitions of the ground state, the excited states and the wetting layer.

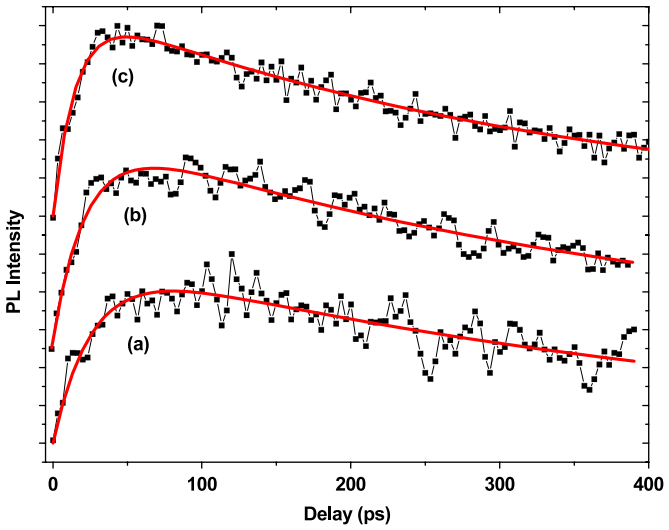

Figure 3. Time evolution of the photoluminescence of InGaAs/GaAs modulation p-doped QDs for the ground state (a), first excited state (b) and second excited state (c) of the QDs at room temperature. Solid lines are fits with an exponential rise and decay function.

25 and 18 ps, and decay times of 445, 390 and 340 ps, respectively. At high excitation, the PL evolution exhibits a non-exponential plateau, which has been attributed to the state filling effect according to calculations and observations [6, 18].

For p-doped QDs, the lowest few levels of the valence band are occupied prior to optical excitation. Basically, electrons are excited into the GaAs barrier under laser excitation of 800 nm because the photon energy is larger than the band gap of the GaAs barrier. These photoexcited electrons then relax quickly into the low levels of the barrier and the InGaAs WL

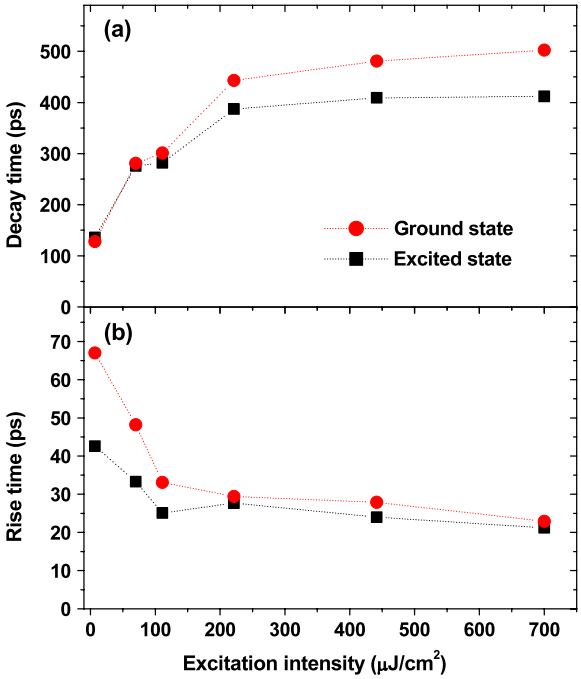

Figure 4. Rise time (a) and decay time (b) as a function of excitation intensity in modulation p-doped InGaAs/GaAs QDs. The circles and squares represent the ground state and excited state, respectively.

through effective longitudinal optical (LO) phonon scattering. Electrons can be captured from the WL directly into the ground state of the QDs or first captured into the excited state of the QDs below the WL, and then they relax into the ground state of the QDs [19]. The dominant relaxation channel for p-doped QDs is electron–hole scattering [4, 20]. In this process electrons release their excess energy through scattering with holes built in the valence band of the QDs. The hole energy states in the valence band are closely spaced and strongly broadened by phonon scattering, thereby providing a wide phase space of available energy-conserving transitions.

The PL evolution was measured at room temperature with various excitation intensities and fitted with an exponential rise and decay function. Figure 4 compares the rise times and decay times of the ground state and first excited state as a function of excitation intensity. The rise times of the ground state and excited state show a similar trend: for example, fairly long rise times of 60 and 40 ps appear at very low excitation intensity. The rise times decrease with increasing excitation intensity until about 100 μJ cm^{-2}, where the rise times are 30 ps and 25 ps for the ground state and excited state, respectively. With further increase of excitation intensity, however, the rise times do not show a further decrease.

In the low excitation regime the scattering between photoexcited electrons and excess holes built in the valence band due to p-doping is the dominant mechanism for the relaxation from the wetting layer into the QDs [2, 13]. The electron states of the QDs are rarely occupied and thus the state filling effect plays only a little role. At low excitation, the density of photoexcited electrons in the WL is very low, so the rate of the electron–hole scattering is very low, and thus a long rise time is observed. With increasing excitation intensity the density of photoexcited electrons increases, and thus the electron–hole scattering is enhanced, which leads to a decrease of the rise time. With increasing excitation intensity, however, the occupied density of electrons

in the QD states increases as well. The state filling effect plays an increasing role, which results in a reduced relaxation channel. With further increase of excitation, the state filling effect becomes the dominant mechanism and thus the rise time does not decrease further. Therefore, in the low excitation regime, the rise time decreases with excitation intensity due to enhancement of the electron–hole scattering, whereas in the high excitation regime the state filling effect results in a hindered relaxation and thus a flat variation in the rise time.

The decay time, in principle, is determined mainly by radiative and nonradiative recombination. Intersubband relaxation gives a limited contribution to the excited states because it is not very effective in this particular doped sample on account of the quite close decay times in the ground-state and excited-state transitions [21]. For a doped sample, the nonradiative centres are most likely the defects introduced by the doping, and these have a relatively short lifetime [22, 23]. At low excitation, nonradiative centres play the main role, and thus a short decay time is obtained. With increasing excitation, the nonradiative channel appears to saturate due to the low density of the defects. Radiative recombination becomes the dominant mechanism and thus a long decay is observed.

We present a simplified rate equation model in order to understand quantitatively the main microscopic processes involved in the observed PL in modulation doped QDs [24, 25]. The PL intensity of a transition is proportional to the number of respective electron–hole pairs. For a p-doped QD discrete level system, the PL intensity for transition i is proportional only to the electron density N_i in the level i of the conduction band due to the excess built-in holes in the QD region prior to the excitation. The electron levels can be made to have an energy spacing as large as 80 meV, while the hole levels are much more closely spaced at 5–10 meV [26, 27]. The closely spaced hole levels result in thermal smearing of the hole population among many hole states. In this situation, the electrons have a high probability of residing in the ground level of the QDs and the injected electrons easily find holes with which to recombine due to the excess built-in hole population. Thus the transition energy difference corresponds to the energy spacing of the electrons, and the carrier capture is mostly related to electrons.

The carrier relaxation from j to i ($j > i$) is proportional to the non-occupancy of the level. The rate equation for level i can then be written [24]:

$$\frac{\mathrm{d}N_i(t)}{\mathrm{d}t} = -\frac{N_i(t)}{\tau_{\mathrm{el}}^i} + \sum_{j>i} \frac{N_j(t)}{\tau_{\mathrm{rel}}^{ji}} \frac{D_i - N_i(t)}{D_i} - \sum_{j<i} \frac{N_i(t)}{\tau_{\mathrm{rel}}^{ij}} \frac{D_j - N_j(t)}{D_j} + G_i(t) \tag{1}$$

where τ_{el}^i is the effective lifetime of the ith level, τ_{rel}^{ij} and τ_{rel}^{ji} are relaxation times between the ith and jth level of the electrons, D_i is the state density, and $G_i(t)$ is the population captured from the WL, which can be expressed as $\frac{\eta\sigma N_0 I_{\mathrm{ex}}}{\tau_{\mathrm{cap}}^i} \frac{D_i - N_i(t)}{D_i}$, where τ_{cap}^i is the capture time, σ is the absorption cross section, I_{ex} is the laser intensity, N_0 is the total state density in the wetting layer, and η is the capture efficiency. The factor $[D_i - N_i(t)]/D_i$ is a state filling factor which takes account of the fact that the electron can only relax to a lower-lying unoccupied dot level (Pauli blocking).

For the modulation doped QDs, electron relaxation from the WL is the dominant channel, while intersubband relaxation plays only a minor role in the energy relaxation. It is reasonable to neglect the intersubband relaxation in equation (1), and the rate equation can then be written in the simple form

$$\frac{\mathrm{d}N_i(t)}{\mathrm{d}t} = -\frac{N_i(t)}{\tau_{\mathrm{el}}^i} + \frac{\eta\sigma I N_0}{\tau_{\mathrm{cap}}^i} \frac{D_i - N_i(t)}{D_i}. \tag{2}$$

At the maximum point of population $N(t = t_{\mathrm{m}})$, the peak of the PL evolution, $\mathrm{d}N_i(t_{\mathrm{m}})/\mathrm{d}t = 0$, is satisfied. Thus the population of level i is found to be

$$N_i(t = t_{\mathrm{m}}) \propto D_i/(1 + \alpha_i D_i/I), \tag{3}$$

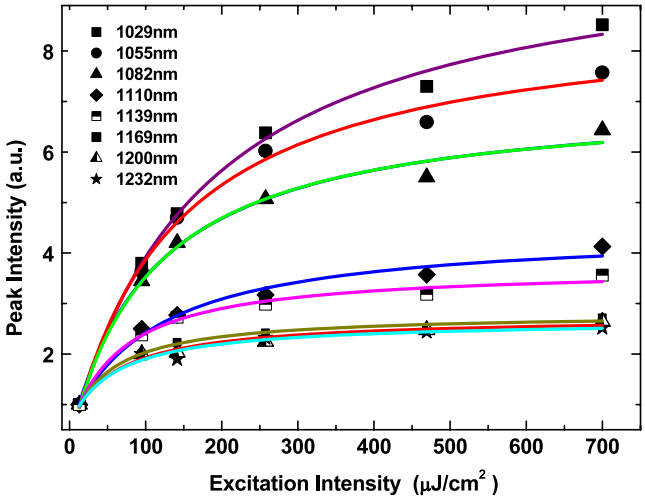

Figure 5. Peak intensity dependence of the excitation intensity at different detection wavelengths. The solid lines represent fits using $I_{\mathrm{PL}} = A/(1 + B/I_{\mathrm{ex}})$, with B the saturation factor.

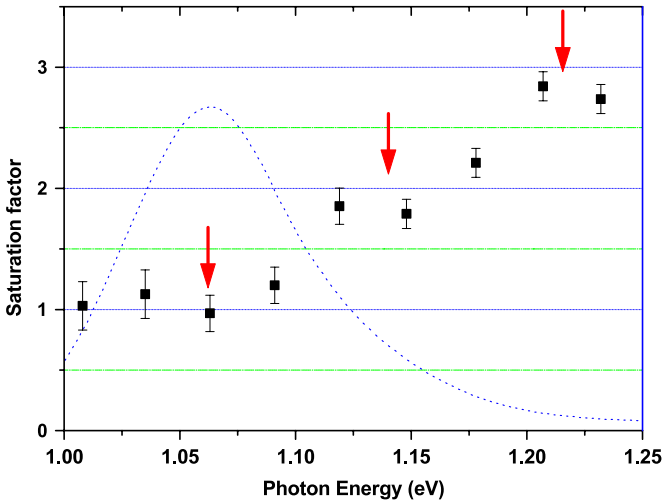

Figure 6. Saturation factor as a function of photon energy deduced from the time-resolved photoluminescence for the modulation p-doped InGaAs quantum dots. The arrows indicate the energy of the lowest three states of the QDs and the dotted curve is the corresponding PL curve.

where $\alpha_i D_i$ is a saturation factor which depends on the level, and $\alpha_i = \tau^i_{\mathrm{cap}}/(\sigma N_0 \tau^i_{\mathrm{el}})$. The corresponding intensity at the maximum point is given by

$$I^i_{\mathrm{max}}(I_{\mathrm{ex}}) \propto \eta_i N_i \propto \eta_i D_i/(1 + \alpha_i D_i/I_{\mathrm{ex}}), \tag{4}$$

where η_i is the quantum efficiency.

We measure the excitation intensity dependence of the PL at different detection wavelengths and extract the peak intensity from the fitted curves, as plotted in figure 5. It is evident that a significantly different saturation occurs for the different wavelengths. In order to compare the saturation characteristics we fit the curves with equation (4) and deduce the saturation factor as a function of detection energy, as shown in figure 6.

The potential function of the QDs can be described by the expression $V_j = m^*\omega_j^2 r^2/2$ using a harmonic oscillator model for parabolic quantum confinement [28], where j represents an electron or a hole and m^*, ω_j and r are the effective mass, the frequency and the radial coordinate of the dots, respectively. The eigenenergies for a single electron or hole are given by $E_{\mathrm{lm}}^j = \hbar\omega_j(2\ell+m+1)$, where ℓ and m are the radial and angular momentum quantum numbers, and $\hbar$ is Planck's constant. The eigenenergies can also be written as $E_{\mathrm{lm}}^j = \hbar\omega_j(i+1)$, setting $i = 2\ell + m$. The degeneracy of each state is $g_i = 2(i+1)$ with $i = 0, 1, 2, \ldots$ when taking the spin degeneracy into account.

The saturation factor $\alpha_i D_i$ increases with detection photon energy. We can estimate the ratio $(\tau_{\mathrm{cap}}/\tau_{\mathrm{el}})_{i=0,1,2}$ for the first three levels based on the excitation dependent experiments: τ_{cap} is the rise time in the low excitation regime, and thus with minimal state filling effect; and τ_{el} is the decay time in the high excitation regime, where the electron–hole recombination makes the dominant contribution. Thus we can get the relation $(\tau_{\mathrm{cap}}/\tau_{\mathrm{el}})_{i=0}{:}(\tau_{\mathrm{cap}}/\tau_{\mathrm{el}})_{i=1}{:}(\tau_{\mathrm{cap}}/\tau_{\mathrm{el}})_{i=2} \approx 1{:}0.9{:}0.8$, with $i = 0$ for the ground level. We can then deduce the ratio of the saturation factor of the excited states to the ground state, $(\alpha_i D_i)_{i=2}{:}(\alpha_i D_i)_{i=1}{:}(\alpha_0 D_0)_{i=0} \approx 2.5{:}1.8{:}1.0$. Taking into account the inhomogeneous broadening of the QD ensemble due mainly to fluctuations in dot size, the saturation factor should increase with increasing detection photon energy.

The saturation factors deduced from the excitation intensity dependence experiment are shown in figure 6 (squares). The dotted line is the PL curve and the arrows indicate the locations of the lowest three transitions according to the CWPL experiment. It is evident that the saturation factor increases with increasing detection energy, which is consistent with the prediction of the rate equations.

4. Summary

We have studied the state filling effect and electron dynamics in modulation p-doped InGaAs/GaAs self-assembled quantum dots using time-integrated and time-resolved up-conversion photoluminescence. A significant state filling effect is found with exclusion of the phonon bottleneck effect, and the rise times and decay times vary with the excitation intensity. In the low excitation regime, the dominant relaxation from the wetting layer to the quantum dots is scattering between the photoexcited electrons and excess holes in the valence band due to doping, and thus the rise time decreases with increasing excitation. In the high excitation regime, the state filling effect plays a dominant role, and thus results in a flat variation of rise times. A simplified rate equation model indicates that the modulation p-doped quantum dots exhibit an increasing saturation factor with increasing detection photon energy based on the theory of parabolic confinement of the quantum dots, which is consistent with the observed excitation dependence.

Acknowledgments

This work was supported by an Australian Research Council Discovery grant and a Swinburne University Strategic Initiative grant. XMW acknowledges partial financial support of the Chinese National Natural Science Foundation (10364004) and the Yunnan Natural Science Foundation (2003E0013M).

References

[1] Deppe D G, Huang H and Shchekin O B 2002 *IEEE J. Quantum Electron.* **38** 1587
[2] Gündoğdu K, Hall K C, Boggess T F, Deppe D G and Shchekin O B 2004 *Appl. Phys. Lett.* **85** 4570

[3] Shchekin O B, Ahn J and Deppe D G 2002 *Electron. Lett.* **38** 712
[4] Urayama J, Norris T B, Singh J and Bhattacharya P 2001 *Phys. Rev. Lett.* **86** 4930
[5] Osborne S, Blood P, Smowton P, Lutti J, Xin Y C, Stintz A, Huffaker D and Lester L F 2004 *IEEE J. Quantum Electron.* **40** 1639
[6] Raymond S, Fafard S, Poole P J, Wojs A, Hawrylak P, Charbonneau S, Leonard D, Leon R, Petroff P M and Merz J L 1996 *Phys. Rev.* B **54** 11548
[7] Grundmann M, Heitz R, Ledentsov N, Stier O, Bimberg D, Ustinov V M, Kopev P S, Alferov Z I, Ruvimov S S, Werner P, Gosele U and Heydenreich J 1996 *Superlatt. Microstruct.* **19** 81
[8] Yang W D, Lee H, Johnson T J, Sercel P C and Norman A G 2000 *Phys. Rev.* B **61** 2784
[9] Nielsen T R, Gartner P and Jahnke F 2004 *Phys. Rev.* B **69** 235314
[10] Schneider H C, Chow W W and Koch S W 2001 *Phys. Rev.* B **64** 115315
[11] Bockelmann U and Egeler T 1992 *Phys. Rev.* B **46** 15574
[12] Heitz R, Veit M, Ledentsov N N, Hoffmann A, Bimberg D, Ustinov V M, Kopev P S and Alferov Z I 1997 *Phys. Rev.* B **56** 10435
[13] Siegert J, Marcinkevicius S and Zhao Q X 2005 *Phys. Rev.* B **72** 085316
[14] Li X Q, Nakayama H and Arakawa Y 1999 *Phys. Rev.* B **59** 5069
[15] Schaller R D, Pietryga J M, Goupalov S V, Petruska M A, Ivanov S A and Klimov V I 2005 *Phys. Rev. Lett.* **95** 196401
[16] Mukai K, Ohtsuka N, Shoji H and Sugawara M 1996 *Phys. Rev.* B **54** R5243
[17] Dao L V, Gal M, Carmody C, Tan H H and Jagadish C 2000 *J. Appl. Phys.* **88** 5252
[18] Park Y M, Park Y J, Kim K M, Shin J C, Song J D, Lee J I and Yoo K H 2004 *J. Cryst. Growth* **271** 385
[19] Nielsen T R, Gartner P and Jahnke F 2004 *Phys. Rev.* B **69** 235314
[20] Sosnowski T S, Norris T B, Jiang H, Singh J, Kamath K and Bhattacharya P 1998 *Phys. Rev.* B **57** R9423
[21] Adler F, Geiger M, Bauknecht A, Scholz F, Schweizer H, Pilkuhn M H, Ohnesorge B and Forchel A 1996 *J. Appl. Phys.* **80** 4019
[22] Siegert J, Marcinkevicius S, Fu L and Jagadish C 2006 *Nanotechnology* **17** 5373
[23] Shchekin O B and Deppe D G 2002 *Appl. Phys. Lett.* **80** 2758
[24] Grosse S, Sandmann J H H, von Plessen G, Feldmann J, Lipsanen H, Sopanen M, Tulkki J and Ahopelto J 1997 *Phys. Rev.* B **55** 4473
[25] Van Dao L, Wen X M, Do M T T, Hannaford P, Cho E C, Cho Y H and Huang Y D 2005 *J. Appl. Phys.* **97** 013501
[26] Sheng W D and Leburton J P 2002 *Appl. Phys. Lett.* **80** 2755
[27] Stier O, Grundmann M and Bimberg D 1999 *Phys. Rev.* B **59** 5688
[28] Grundmann M and Bimberg D 1997 *Phys. Rev.* B **55** 9740